Alkyl-templated cocrystallization of long-chain bromoalkanes by lipid-like ionic liquids

SCHOLARONE™
Manuscripts

Alkyl-templated cocrystallization of long-chain 1-bromoalkanes by lipid-like ionic liquids

Muhammadiqboli Musozoda,[a] Joseph Muller II,[b] Grace I. Anderson,[b] Mairead Boucher,[c] Matthias Zeller,[d] Casey C. Raymond,[a] Patrick C. Hillesheim,*[c] Arsalan Mirjafari*[a]

The serendipitous discovery of an unorthodox ionic cocrystallization system using 2-mercaptothiazolium-based ionic liquids as a crystallization milieu paves the way for the first report of crystal structures of long-chain 1-bromoalkanes. We used single crystal X-ray diffraction to determine the structures of 1-bromo-hexadecane and 1-octadecane with the aid of ionic liquids with alkyl side chains of equivalent length to the bromoalkane at room temperature. Long alkyl chains in combination with σ-hole interactions from strategically placed sulfur motifs synergistically function to crystallize the 1-bromoalkanes.

More than two decades ago, a general strategy was proposed for the development of ionic liquids (ILs) as alternative solvent systems for diverse classes of solutes, including cellulose,[1] greenhouse gases,[2] lithium salts,[3] nucleic acids,[4] and active pharmaceutical ingredients.[5] While significant progress was made to develop novel functional ILs, their usefulness as crystallization solvents/additives is rarely explored with a few notable exceptions.[7–11] Despite these successes, the lack of literature on this topic can be attributed to the intrinsic design of ILs that prevents them from crystallizing. This characteristic is coupled with their non-volatility, high viscosity, and strong dissolving capabilities, further contributing to the scarcity of relevant studies.[12]

Lipid-like (or lipid-inspired) ILs were introduced as low-melting salts with structural features similar to natural lipids, *i.e.,* imidazolium headgroups to which a long saturated or unsaturated hydrocarbon tails are appended, enabling high lipophilicity while retaining melting points (T_m) near ambient

temperatures.[13] In this endeavor, we found that the use of *ene*,[14] thioether,[15] and cyclopropyl[16] moieties integrated into long aliphatic tails of imidazolium-type ILs causes a change that disrupts side-chain packing, resulting in reduced T_m values relative to otherwise identical analogs with saturated tails.

As part of a larger effort to design and prepare lipid-like ILs as safe and effective gene delivery vectors,[17] we subsequently aimed to create ILs with improved fluidity and chemical stability that are potentially biocompatible while maintaining lipophilic characteristics. Because of the presence of the endocyclic sulfur atom, we chose 2-mercaptothiazole (**1**) and 2-mercapto-2-thiazoline (**2**) as heterocyclic moieties. The synthetic strategy was based on the double alkylation of **1** and **2** with long chain alkyl/alkenyl halides to prepare new liposome-like salts (**3**-m:n, **4**-m:n*;* where *m* and n are the numbers of carbons and double bonds on tails), containing saturated and *cis*-unsaturated C_{16} and C_{18} tails (Scheme 1).
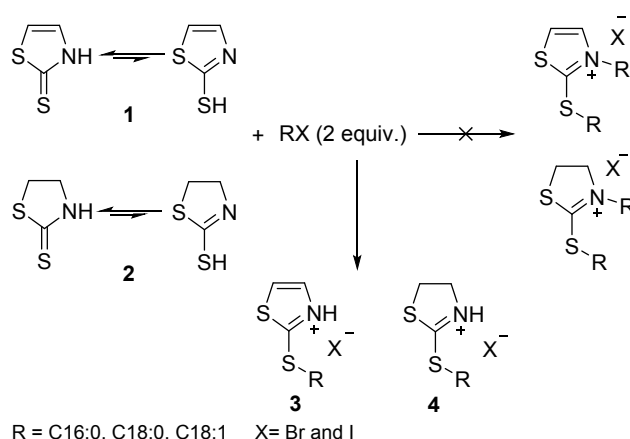
Scheme 1. Synthesis of ILs **3** and **4**. The most stable tautomers of compounds **1** and **2** are when the exocyclic sulfur atoms are unprotonated (2-thione forms).

After slow evaporation of the solvent at room temperature for 6-10 weeks from a mixture of acetonitrile/methanol (9:1 ratio), needle-shaped crystals suitable for X-ray diffraction were

[a] *Department of Chemistry, State University of New York at Oswego, Oswego, New York 13126, USA. E-mail: arsalan.mirjafari@oswego.edu*

[b] *Department of Chemistry and Physics, Florida Gulf Coast University, Fort Myers, Florida 33913, USA*

[c] *Department Chemistry and Physics, Ave Maria University, Ave Maria, Florida 34142, USA. E-mail: patrick.hillesheim@avemaria.edu*

[d] *Department of Chemistry, Purdue University, West Lafayette, Indiana 47907, USA*

formed. According to the integration data of the ^{1}H NMR analysis of the formed crystals, we initially postulated that the synthesized compounds were the double-substituted. Unexpectedly, the crystal structure instead showed a molecule of saturated 1-bromoalkane cocrystallized with **3**-16:0 and **3**-18:0 ILs as white solids through a host-guest cocrystallization effect (Figure 1). Generally, obtaining diffraction quality single crystals of long chain haloalkanes is challenging mostly due to their low T_m values and presence of multiple conformations and rotational isomers of the hydrocarbon chains. To our knowledge, crystal structures have not been reported for 1-bromohexadecane, 1-bromooctadecane, or related long-chain mono-bromoalkanes, making this the first report of IL-induced amorphous-to-crystalline transformation of long-chain alkyl bromides. The cocrystals of 1-bromooctadecane were obtained with the aid of the IL **3**-C18:0 (Figure 1). The resultant cocrystal displays several notable characteristics, which help to explain the observed cocrystallization phenomena for these systems.
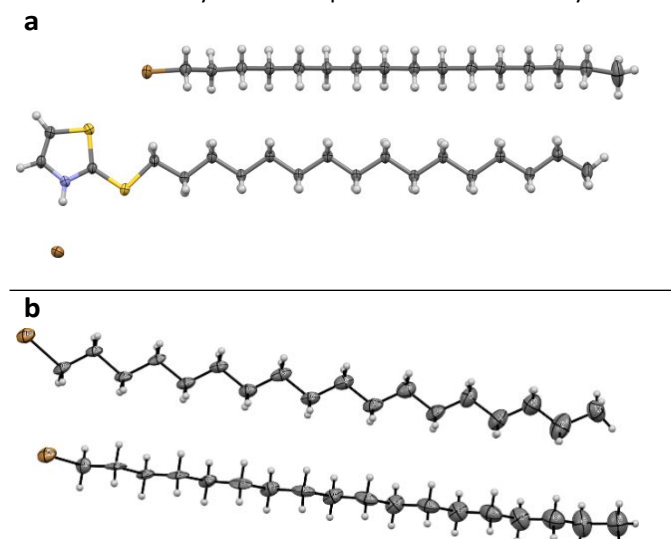

Figure 1. a) Asymmetric unit of **3**-16:0 crystallized with 1-bromohexadecane shown with 50% probability ellipsoids. b): Asymmetric unit of 1-bromooctadecane, crystallized with the aid of **3**-18:0.

To validate the effectiveness of the host-guest system, we attempted to grow suitable crystals of the alkyl bromides without the presence of the corresponding IL using identical solvent systems and crystallization methods. Despite considerable efforts, we could not produce any crystalline solids, much less any diffraction quality crystals. The system is very sensitive with regard to chain length and geometry of 1-bromoalkane and IL cation: The crystallization approach was ineffective in affording all of the complexes reported in Scheme 1, except for **3**-16:0 and **3**-18:0. Expectedly, the ILs with *cis*-chain unsaturation, **3**-16:1 and **3**-18:1, did not show crystalline behavior, following our prior observations that olefin-containing ILs are less densely packed.[16] We were unable to crystallize **4** due to poor chemical stability, leading to slow hydrolysis of the iminium moiety during crystallization process (Figures S1-S4). We did not observe any hydrolysis of IL **3**.

Fortified by these results, we reviewed the chemical literature to determine the scope and nature of prior research at the nexus of salts and haloalkanes and found a considerable number of reports pertaining to the formation of Langmuir monolayers. Extensive studies on the characterizations, properties, and molecular arrangement of Langmuir monolayers consisting of amphiphiles such as fatty acids and esters, and nonamphiphilic materials long-chain bromoalkanes are well-documented.[18] However, only a handful of reports exist on the study of their two-dimensional crystalline properties with X-ray diffraction or reflection techniques, using synchrotron sources and neutron scattering.[18] While the *crystallinity* of the Langmuir monolayers was established by these techniques, to our knowledge, their unambiguous *single-crystal* structures have been not reported.

Long chain 1-bromoalkanes are incapable of forming monolayers by themselves at the air–water interface; however, they can be incorporated to improve the surface compatibility of fatty acids/esters and form stable thin films.[20] This strategy requires the design of two substances that act synergistically to promote self-assembly. The amphiphilic ILs (**3**) control the critical intermolecular spacing and serve as a host for the second molecule, the non-polar *n*-alkyl bromide guests. Like Langmuir monolayers, our materials are arranged so that like groups are adjacent to each other (Figure 2). Cohesion occurs *via* van der Waals interactions between the long-chain alkyl tails in the hydrophobic domain and through strong, charge-assisted H-bonding in the hydrophilic domain. The structure balances two conflicting intermolecular interactions: long chains which aim to pack in parallel to maximize the lateral hydrophobic interactions, and cationic headgroups which align to optimize N–H^{+}···Br^{−} hydrogen bonding, leading to the formation of an ionic, hydrophilic bilayer.
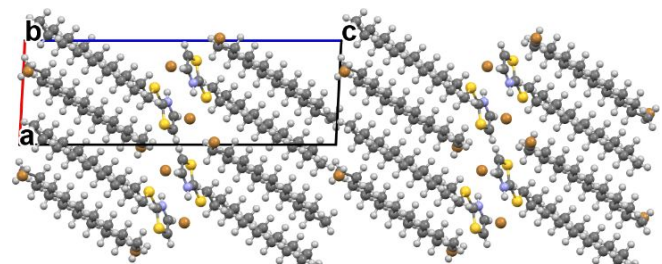

Figure 2. Packing diagram of compound **3**-16:0. Packing diagram viewed down the crystallographic b axis.

We hypothesize that this cocrystallization phenomenon is aided, in part, by the formation of chalcogen bonds, a distinctive non-bonding interaction arising from the electron-deficient sulfur atom and electron-rich bromine atoms. Chalcogen bonds, a specific kind of σ-hole interaction, are well-established supramolecular synthons, helping direct structure and reactivity within biologically pertinent thiazolium-based systems, *e.g.,* Vitamin B1.[21]

To test the validity of our hypothesis, we took a closer look at the crystals and examined the intermolecular forces between the components. There are four relevant S···Br contacts in the crystals of **3**-16:0. Both the endo and exocyclic sulfur atoms each form two interactions: one with the bromine and one with the Br^{−} anion. The two interactions with the exocyclic sulfur (S2) are at distances of 3.6695(9) Å (d(S2···Br2A^i, i = -1+x, +y, +z) and 4.0581(8) Å ((d(S2···Br1)). The heterocyclic sulfur (S1) makes a

slightly longer interaction with the alkyl bromide at 3.786(1) Å (d(S1···Br2A)). Finally, S1 also interacts with a symmetry adjacent anion Br1[j] at a distance of 3.7685(9) Å (d(S1···Br1[j], j = 1+x, +y, +z). Figure S5 depicts these interactions, which are near the sum of the radii of the respective atoms, within the expected ranges observed in crystals.[22]

Notably, the angles of the interactions are crucial for chalcogen bond formation. For **3**-16:0, the angles for the interactions with the aromatic sulfur are 136° and 153° (∠ C5—S1···Br2A & C2—S1···Br1, respectively) and an angle of 144° for the exocyclic sulfur (∠ C2—S2···Br2A[i]). Although these angles are less than the idealized ranges of ~160–180°,[23] they are not outside the range of contacts observed in related systems,[21] reported in the CSD.[24] The final chalcogen bond, however, has an angle of 177° (∠ C5—S2···Br1). The less-than-ideal angles would lead to weaker interactions and thus could rationalize the difficulty in crystallization of **3**-16:0 and the observed disorder within its crystal (head-tail disorder of the bromoalkene, disordering the terminal methyl and bromine atoms). Further, the disorder also emphasizes the more dominant H···H interactions from the alkyl chains with respect to a major driving force for crystallization, though coulombic interactions are still a major contributing factor.

We used Hirshfeld surface analysis to gain deeper understanding of the interactions present within the crystal (Figure 3). There are numerous non-covalent interactions not directly involving the host–guest systems, as would be expected for such a structure. In brief, the H···H interactions comprise the highest percentage of the intermolecular interactions in **3**-16:0 at 79.3%. Additionally, a prominent green streak is observed from d_i/d_e ≈ 1.8 – 2.2 Å. This streak represents S···Br interactions within the crystals. For **3**-16:0 this comprises 3.5% of the total interactions. Additional S···H interactions comprise 2.6% of the close-contacts within the crystals. The S···H interactions are well established as stabilizing contacts within biological systems.[25]

The cationic heterocycles of symmetry adjacent moieties arrange in parallel offset π-stacking interactions wherein the thioether moiety (S2) resides above the nitrogen (N3). The S···N distance is 3.522(3) Å (d(S2···N3[k], k = 1-x, 3-y, 1-z) and the S2···centroid distance is 3.5571(8) Å. This interaction helps show the anisotropic electron distribution of the sulfur giving rise to different stabilizing interactions, $i.e.,$ S···Br versus S···π.[26] This stacking interaction is facilitated by the planar arrangement of the heterocycle and the thioether tail with a N3—C2—S3—C6 torsion angle of 177.1(3) Å, establishing a set of H···H alkyl interactions between planes along the crystallographic c axis.

Thus, speculatively, the chalcogen and the H-bonds are synergistic interactions, leading to the formation of the cocrystal with the H-bonds stabilizing the planar arrangement of neighboring IL moieties and the chalcogen bonds facilitating the close-packing of the 1-bromoalkane and the tethered thioether moiety. This point can be emphasized when examining the crystal structure of IL **3**-18:0. While the alkyl chain of **3**-18:0 is slightly longer than that of **3**-16:0, the molecular structures are nearly identical (Figure 4).
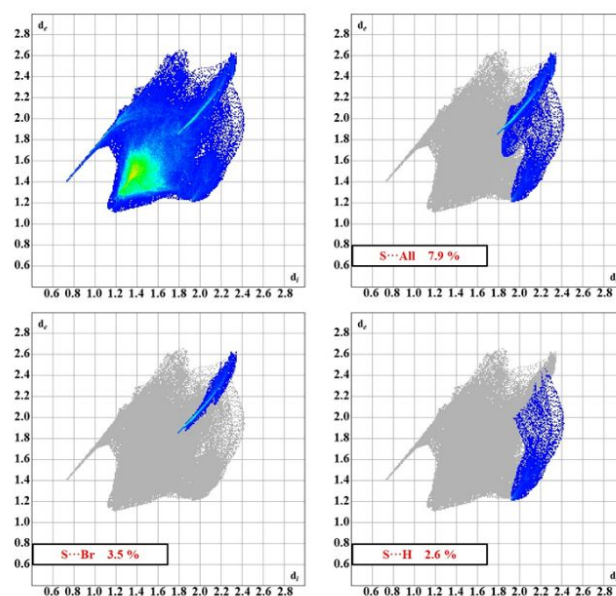

Figure 3. Fingerprint plots showing interactions with the sulfur atoms within the crystal of **3**:16-0.

Examining a packing diagram for **3**-18:0 reveals interdigitation of the alkyl chains assisted by the formation of N—H···Br bonds, which allows for contact between the hydrophobic domains (Figure 5-**I**). If one examines a plane of **3**-18:0 formed simply by the H-bonding, a hydrophobic 'pocket' is observed between the alkyl chains. For **3**-16:0, the interdigitation is replaced, instead, by the alkyl bromide chain (Figures 5-**II** and 5-**III**). The alkyl bromide moiety acts as a substitute source of alkyl-alkyl interactions while also forming chalcogen bonds, leading to the growth of the cocrystal. Thus, the IL-bound alkyl chains act as a template, stabilized via H-bonding, allowing the alkyl bromides to replace the
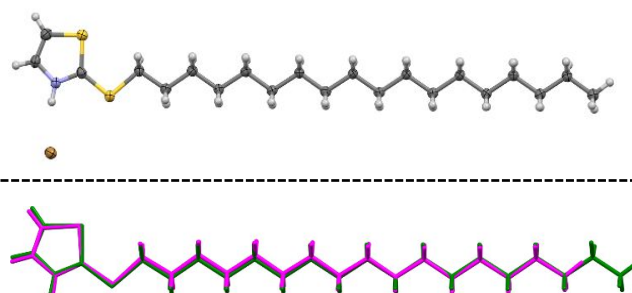

interdigitated structure from the pure compound.

Figure 4. Top: Asymmetric unit of **3**-18:0 shown with 50% probability ellipsoids. Bottom: Overlay of asymmetric units for **3**-16:0 (pink) and **3**-18:0 (green).

To further rationalize this observation, we characterized the solution-crystallized complexes with differential scanning calorimetry (DSC) and the obtained data was shown in Table S2 and Figure S6 (see ESI). The pure ILs **3** display distinctive, relatively low T_m peaks. Once again, nature's strategy of modulating T_m in lipidic materials has an analogous effect when applied to ILs. It is clear from the forgoing data that the IL **3**/R—Br (R = C_{16}, C_{18}) complexes are crystalline and are consistent with a 1:1 stoichiometric ratio based on the values of the enthalpy changes. The crystallized samples display the correct

overall compositions. As noted, similar long-chain compounds (*e.g.,* fatty acids/esters), lipid-like IL systems exhibit stepwise melting behavior, thermotropic polymorphism, and thermally induced solid-solid phase transitions before complete melting occurs.[15] The overall characteristics of the DSC curves manifest comparative, stepwise T_m behaviors relative to the pure samples. Such a high enthalpy change (strong solid/liquid transitions) are indicative of solid states in which the
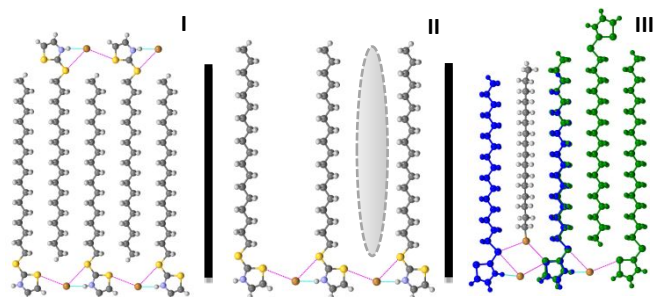
interbilayer interactions are maximized.

Figure 5. (I) Packing of **3**:18-0 showing interdigitated alkyl chains. (II) Formation of a plane *via* the H-bonds, leaving templated voids by the alkyl groups. (III) Overlay of packing for **3**-16:0 cocrystal (blue) and **3**-18:0 (green), illustrating how the bromolkanes fits within the templates. H-bonds are shown in cyan and chalcogen bonds in magenta (dotted lines). The gray shape with purple highlights indicates the hydrophobic pocket.

For comparison, we prepared the complexes with identical compositions from the melt. We noted that the phase behaviors of **3**-16:0/1-bromohexadecane and **3**-18:0/1-bromooctadecane complexes prepared *via* crystallization and in the melt were very similar. However, biphasic behavior near the melting points of the molten samples was detected, indicative of marginally incomplete formation of host-guest complexes. It is likely that the supramolecular integrity is not perfect in the case of molten samples due to the lack of mobility, rationalizing the inconsistent pattern observed in the thermal behavior of the molten samples.

In summary, this work describes a debut example of a cocrystal assembled from long-chain bromoalkanes and ion pairs delivered by the 2-mercaptothiazolium-based ILs. The novel structures are formed from unique host–guest complexes, which pack into a lipid-like bilayer. We reproducibly obtained crystalline materials of the crystallized IL/RBr complexes from the experimental setup described herein. We verified the crystal compositions by SC-XRD for three samples, affirming the consistency of the obtained data (see the ESI for details). The unique structures of complexes resemble that of biomembranes and present an opportunity for IL supramolecular chemistry, opening new avenues to design tailored materials with applications in selective and sustainable haloalkane separations, and the crystallography of Langmuir monolayers. Studies aimed at assessing an array of possibilities to achieve precise crystal engineering techniques *via* tailored ILs that guarantee the specific crystallization outcomes are in progress in our laboratories.

Conflicts of interest

There are no conflicts to declare.

Notes and references

1 H. Wang, G. Gurau and R. D. Rogers, *Chem. Soc. Rev.*, 2012, **41**, 1519–1537.
2 S. Zeng, X. Zhang, L. Bai, X. Zhang, H. Wang, J. Wang, D. Bao, M. Li, X. Liu and S. Zhang, *Chem. Rev.*, 2017, **117**, 9625–9673.
3 M. Watanabe, M. L. Thomas, S. Zhang, K. Ueno, T. Yasuda and K. Dokko, *Chem. Rev.*, 2017, **117**, 7190–7239.
4 K. S. Egorova, A. V. Posvyatenko, S. S. Larin and V. P. Ananikov, *Nucleic Acids Res.*, 2021, **49**, 1201–1234.
5 X. Wu, Q. Zhu, Z. Chen, W. Wu, Y. Lu and J. Qi, *J. Control. Release*, 2021, **338**, 268–283.
6 M. B. Shiflett, Ed., *Commercial Applications of Ionic Liquids*, Springer International Publishing, 2020.
7 D. A. Fowler, S. J. Teat, G. A. Baker and J. L. Atwood, *Chem. Commun.*, 2012, **48**, 5262–5264.
8 D. A. Fowler, J. L. Atwood and G. A. Baker, *Chem. Commun.*, 2013, **49**, 1802–1804.
9 C. C. Weber, S. A. Kulkarni, A. J. Kunov-Kruse, R. D. Rogers and A. S. Myerson, *Cryst. Growth Des.*, 2015, **15**, 4946–4951.
10 Q. Zeng, A. Mukherjee, P. Müller, R. D. Rogers and A. S. Myerson, *Chem. Sci.*, 2018, **9**, 1510–1520.
11 A. Mukherjee, R. D. Rogers and A. S. Myerson, *CrystEngComm*, 2018, **20**, 3817–3821.
12 W. M. Reichert, J. D. Holbrey, K. B. Vigour, T. D. Morgan, G. A. Broker and R. D. Rogers, *Chem. Commun.*, 2006, 4767–4779.
13 S. M. Murray, R. A. O'Brien, K. M. Mattson, C. Ceccarelli, R. E. Sykora, K. N. West and J. H. Davis, *Angew. Chem. Int. Ed.*, 2010, **49**, 2755–2758.
14 A. Mirjafari, R. A. O'Brien and J. H. Davis, in *Ionic Liquids in Lipid Processing and Analysis*, Elsevier, 2016, pp. 205–223.
15 A. Mirjafari, R. A. O'Brien, K. N. West and J. H. Davis, *Chem. Eur. J.*, 2014, **20**, 7576–7580.
16 R. A. O'Brien, P. C. Hillesheim, M. Soltani, K. J. Badilla-Nunez, B. Siu, M. Musozoda, K. N. West, J. H. Jr. Davis and A. Mirjafari, *J. Phys. Chem. B*, 2023, **127**, 1429–1442.
17 D. J. Siegel, G. I. Anderson, L. M. Paul, P. J. Seibert, P. C. Hillesheim, Y. Sheng, M. Zeller, A. Taubert, P. Werner, C. Balischewski, S. F. Michael and A. Mirjafari, *ACS Appl. Bio Mater.*, 2021, **4**, 4737–4743.
18 O. N. Jr. Oliveira, L. Caseli and K. Ariga, *Chem. Rev.*, 2022, **122**, 6459–6513.
19 G. Baskar, A. M. Shanmugharaj, S. Venkatesh and A. B. Mandal, *J. Am. Oil Chem. Soc.*, 2001, **78**, 503–507.
20 A. M. Gonçalves da Silva, J. C. Guerreiro, N. G. Rodrigues and T. O. Rodrigues, *Langmuir*, 1996, **12**, 4442–4448.
21 K. Konidaris, A. Daolio, A. Pizzi, P. Scilabra, G. Terraneo, S. Quici, J. S. Murray, P. Politzer and G. Resnati, *Cryst. Growth Des.*, 2022, **22**, 4987–4995.
22 S. S. Batsanov, *Inorg. Mater.*, 2001, **37**, 871–885.
23 Z. P. Shields, J. S. Murray and P. Politzer, *Int. J. Quantum Chem.*, 2010, **110**, 2823–2832.
24 C. R. Groom, I. J. Bruno, M. P. Lightfoot and S. C. Ward, *Acta Crystallogr. B Struct. Sci Cryst. Eng Mater.*, 2016, **72**, 171–179.
25 H. A. Fargher, T. J. Sherbow, M. M. Haley, D. W. Johnson and M. D. Pluth, *Chem. Soc. Rev.*, 2022, **51**, 1454–1469.
26 J. Y. C. Lim and P. D. Beer, *Chem*, 2018, **4**, 731–783.